Tree Physiology 00, 1–10
doi:10.1093/treephys/tpy015

Methods paper

Testing the plant pneumatic method to estimate xylem embolism resistance in stems of temperate trees

Ya Zhang[1,9], Laurent J. Lamarque[2,3], José M. Torres-Ruiz[2], Bernhard Schuldt[4], Zohreh Karimi[5], Shan Li[1,6], De-Wen Qin[7], Paulo Bittencourt[8], Régis Burlett[2], Kun-Fang Cao[7], Sylvain Delzon[2], Rafael Oliveira[8], Luciano Pereira[8] and Steven Jansen[1]

[1]Institute of Systematic Botany and Ecology, Ulm University, Albert-Einstein-Allee 11, 89081 Ulm, Germany; [2]BIOGECO, INRA, University of Bordeaux, 33615 Pessac, France; [3]EGFV, INRA, University of Bordeaux, 33882 Villenave d'Ornon, France; [4]Albrecht-von-Haller-Institute for Plant Sciences, Göttingen University, 37077 Göttingen, Germany; [5]Department of Biology, Faculty of Science, Golestan University, 36154 Gorgan, Iran; [6]Department of Wood Anatomy and Utilization, Research Institute of Wood Industry, Chinese Academy of Forestry, 100091 Beijing, PR China; [7]Guangxi Key Laboratory of Forest Ecology and Conservation, College of Forestry, Guangxi University, 530004 Nanning, PR China; [8]Department of Plant Biology, Institute of Biology, PO Box 6109, University of Campinas – UNICAMP, 13083-970 Campinas, SP, Brazil; [9]Corresponding author (ya.zhang@uni-ulm.de)

Received November 21, 2017; accepted January 31, 2018; handling Editor Maurizio Mencuccini

Methods to estimate xylem embolism resistance generally rely on hydraulic measurements, which can be far from straightforward. Recently, a pneumatic method based on air flow measurements of terminal branch ends was proposed to construct vulnerability curves by linking the amount of air extracted from a branch with the degree of embolism. We applied this novel technique for 10 temperate tree species, including six diffuse, two ring-porous and two gymnosperm species, and compared the pneumatic curves with hydraulic ones obtained from either the flow-centrifuge or the hydraulic-bench dehydration method. We found that the pneumatic method provides a good estimate of the degree of xylem embolism for all angiosperm species. The xylem pressure at 50% and 88% loss of hydraulic conductivity (i.e., Ψ_{50} and Ψ_{88}) based on the methods applied showed a strongly significant correlation for all eight angiosperms. However, the pneumatic method showed significantly reduced Ψ_{50} values for the two conifers. Our findings suggest that the pneumatic method could provide a fast and accurate approach for angiosperms due to its convenience and feasibility, at least within the range of embolism resistances covered by our samples.

Keywords: angiosperms, bench dehydration, conifers, embolism, flow-centrifuge, pneumatic method, secondary xylem, vulnerability curve.

Introduction

There is convincing and clear evidence for the occurrence of xylem embolism in plants, which implies that functional, water-filled conduits (vessels and tracheids) in xylem tissue become air-filled (e.g., Sperry and Tyree 1988, Tyree and Zimmermann 2002, Choat et al. 2016). There is less agreement, however, about the temporal aspects of drought-induced embolism formation in plants, i.e., whether embolism occurs on a daily basis or is limited to seasonal or extreme drought events in intact stems under natural conditions (Cochard and Delzon 2013, Wheeler et al. 2013, Jacobsen et al. 2014). There are even different interpretations about the frequency of embolism occurrence for the same species growing in a similar environment (e.g., grapevine, Jacobsen and Pratt 2012, Charrier et al. 2016, Hochberg et al. 2017). Discussions about xylem embolism resistance strongly rely on the method that is applied, which makes it important to compare and evaluate different techniques (e.g., Torres-Ruiz et al. 2014, Jansen et al. 2015).

Vulnerability curves characterize the plant vulnerability to xylem embolism and express the relationship between xylem water potential (Ψ, MPa) and embolism (Tyree and Sperry 1989). Over the last decades, various techniques have been

used to construct vulnerability curves depending on how xylem embolism is measured, how water stress is induced and how the water potential is measured (Cochard et al. 2013). The xylem water potential can be measured directly with psychrometers, indirectly determined as the leaf water potential after equilibration, or considered as the centrifuge force applied. Quantifying the degree of embolism by hydraulic measurements is the most commonly used approach, which directly estimates the degree of embolism as the percentage loss of hydraulic conductivity (PLC, %; Crombie 1983, Tyree and Dixon 1986, Sperry et al. 1988). This method may seem to be straightforward, but is destructive and requires sufficient care to obtain stable flow measurements (Espino and Schenk 2011). Problems with hydraulic measurements could be pit membrane clogging, vessel occlusion (e.g., by resin or latex), wound response and an excision artefact (Wheeler et al. 2013, Torres-Ruiz et al. 2015). Alternative techniques such as acoustic emissions detection and X-ray microtomography have the main advantage of being non-destructive and non-invasive, but do not directly measure water transport (Mayr and Rosner 2011, Wolkerstorfer et al. 2012, Cochard et al. 2013, Choat et al. 2016).

Bench dehydration is one of the standard methods to induce xylem embolism at a wide range of xylem water potential values because it allows branches or intact plants to dehydrate naturally at an ambient environment (Sperry 1986, Sperry et al. 1988). However, intensive lab work and a large amount of plant material are required for this technique. Centrifugation techniques induce a centrifugal force and require less time and plant material, but an 'open vessel' artefact may limit the application of this technique on species with vessels that are longer than the branch segment (Li et al. 2008, Cochard et al. 2010, Wang et al. 2014, Torres-Ruiz et al. 2015, 2017). Air-injection uses a double-ended pressure chamber to maintain a target pressure on an inserted stem with two ends protruding out of the chamber (Cochard et al. 1992, 2013, Salleo et al. 1992). While this technique is fast, it is equally challenged by the 'open vessel' artefact (Choat et al. 2010, Ennajeh et al. 2011). The optical method to visualize embolism in leaves and stems provides a relatively fast and reliable method to assess xylem embolism resistance in a non-destructive way (Scoffoni and Jansen 2016, Brodribb et al. 2016*a*, 2016*b*, 2017, OpenSourceOV 2018). Considering the importance of xylem embolism in discussions about large-scale tree mortality (Anderegg et al. 2016) and the potential limitations of various methods for constructing vulnerability curves, there is a need for an artefact-free, easy, field-friendly and fast method that would hasten the assemblage of large and global datasets on xylem embolism resistance (Choat et al. 2012).

Recently, Pereira et al. (2016) proposed a pneumatic method, which is fundamentally different from the hydraulic methods. Vulnerability curves in this study were obtained for 15 species by plotting the xylem pressure vs the amount of air discharged from terminal branch ends, while drought stress was induced using the bench dehydration method. Assuming that the air volume discharged from branches that are subjected to different levels of drought stress is mainly affected by embolism, vulnerability curves could be made, and were found to be largely in agreement with hydraulic methods (Pereira et al. 2016). One major advantage of the pneumatic technique is minimal manipulation of the plant samples, while measuring the amount of gas that can be extracted from samples is less complicated and faster (i.e., <3 min) compared with hydraulic measurements.

Since the species tested by Pereira et al. (2016) were mainly tropical to subtropical, and included species with diffuse-porous wood, this paper aims to validate the pneumatic method for both diffuse-porous and ring-porous species from temperate areas. Moreover, additional conifer species are required to test this method, given that the number of conifers in the study by Pereira et al. (2016) was limited to *Cupressus sempervirens* and *Thuja plicata*. Therefore, we selected 10 temperate tree species, covering eight angiosperm and two gymnosperm species. The pneumatic method was compared with the flow-centrifuge technique for diffuse-porous species and conifers, and with hydraulic measurements after bench dehydration for two ring-porous species (*Fraxinus excelsior* and *Quercus robur*). We expected that the pneumatic method would show similar embolism resistance as the flow-centrifuge method for diffuse-porous species and conifers. It was unclear if the pneumatic method would be suitable for ring-porous species due to the large, earlywood vessels, which are known to remain functional only for 1 year (Ellmore and Ewers 1985, 1986, Cochard et al. 1992, Umebayashi et al. 2010, Sano et al. 2011).

Materials and methods

Plant material

Plant material of eight angiosperm species and two gymnosperm species was collected at Ulm University (Germany) (48° 25'20.3"N, 9°57'20.2"E) and the University of Bordeaux (Table 1) (44°47'55.4"N, 0°36'54.2"W). The species selected were all common trees in the forest surrounding Ulm University and the University of Bordeaux. Vulnerability curve measurements according to the pneumatic method and hydraulic-bench dehydration method were conducted at Ulm University. For the flow-centrifuge method, branches were express-shipped to the University of Göttingen, except for the two gymnosperm species, which were measured with a similar flow-centrifuge set-up at the University of Bordeaux.

The pneumatic method

Stem vulnerability curve measurements of 10 species following the pneumatic method were conducted according to Pereira et al. (2016). Briefly, five branches that were ~50–100 cm long and with a 7–10 mm branch diameter were collected from five

Table 1. List of the 10 species studied with reference to their family classification, the technique applied, xylem pressure at 50% and 88% of the maximum air discharged (Ψ_{50P} and Ψ_{88P}) or at 50% and 88% loss of hydraulic conductivity (Ψ_{50H} and Ψ_{88H}) with standard deviation, vessel porosity and collecting site.

Species	Family	Technique	Ψ_{50} (MPa)	Ψ_{88} (MPa)	Vessel porosity	Collecting site
Alnus glutinosa (L.) Gaertn.	Betulaceae	Pneumatic	−1.6 ± 0.2	−2.3 ± 0.3*	Diffuse-porous	Söflingen, Ulm
		Flow-centrifuge	−1.5 ± 0.1	−1.6 ± 0.1		Botanical Garden, Ulm University
Betula pendula Roth	Betulaceae	Pneumatic	−1.8 ± 0.1	−2.2 ± 0.2	Diffuse-porous	Botanical Garden, Ulm University
		Flow-centrifuge	−2.0 ± 0.1	−2.3 ± 0.1		Botanical Garden, Ulm University
Carpinus betulus L.	Betulaceae	Pneumatic	−3.8 ± 0.5	−5.6 ± 0.6*	Diffuse-porous	Botanical Garden, Ulm University
		Flow-centrifuge	−3.7 ± 0.2	−4.5 ± 0.1		Botanical Garden, Ulm University
Corylus avellana L.	Betulaceae	Pneumatic	−2.1 ± 0.3	−3.6 ± 0.8	Diffuse-porous	Ulm University campus
		Flow-centrifuge	−2.0 ± 0.2	−2.8 ± 0.8		Botanical Garden, Ulm University
Fagus sylvatica L.	Fagaceae	Pneumatic	−2.8 ± 0.4*	−5.1 ± 0.6*	Diffuse-porous	Ulm University campus
		Flow-centrifuge	−3.2 ± 0.2	−3.9 ± 0.3		Botanical Garden, Ulm University
Fraxinus excelsior L.	Oleaceae	Pneumatic	−2.4 ± 0.4	−3.8 ± 0.6	Ring-porous	Botanical Garden, Ulm University
		Hydraulic	−2.7	−3.8		Botanical Garden, Ulm University
Liriodendron tulipifera L.	Magnoliaceae	Pneumatic	−1.4 ± 0.2	−1.9 ± 0.3	Diffuse-porous	Botanical Garden, Ulm University
		Flow-centrifuge	−1.5 ± 0.1	−1.8 ± 0.1		Botanical Garden, Ulm University
Pinus pinaster Aiton	Pinaceae	Pneumatic	−2.8 ± 0.2*	−3.8 ± 0.6*	Tracheids only	University of Bordeaux
		Flow-centrifuge	−3.7 ± 0.2	−4.3 ± 0.3		University of Bordeaux
Pinus sylvestris L.	Pinaceae	Pneumatic	−2.0 ± 0.4*	−4.0 ± 0.8	Tracheids only	Botanical Garden, Ulm University
		Flow-centrifuge	−3.2 ± 0.2	−3.7 ± 0.3		University of Bordeaux
Quercus robur L.	Fagaceae	Pneumatic	−3.2 ± 0.3*	−4.4 ± 0.5*	Ring-porous	Ulm University campus
		Hydraulic	−2.8	−3.2		Botanical Garden, Ulm University

Hydraulic = hydraulic-bench dehydration. Standard deviation values in the hydraulic-bench dehydration technique were not available for *F. excelsior* and *Q. robur*. Data with * showed a significant difference ($P < 0.05$) between the techniques applied (for details see Table 2).

adult trees per species. Samples were collected during the early morning between June and September 2016 and 2017. After wrapping the branches in wet tissue and black plastic bags, samples were brought to the lab, re-cut under water and rehydrated for 1 h. The distal end of a branch was then connected to a pneumatic apparatus through a three-way stopcock, which included a syringe as a vacuum source and a pressure sensor (PX26-015GV, Omega). This pressure sensor is not an oil-filled transducer and is designed for working with liquids. For gases, however, the PX140 series was used by Pereira et al. (2016). Comparison of the PX140 and PX26 pressure sensors showed a perfect agreement for air pressure measurements ($R^2 = 1$; $y = -24.602x + 30.69$), indicating that both sensors are suitable for the pneumatic method.

Once the branch end was connected to the pneumatic tubing system, the tubing was not replaced and the branch ends were not shaved before a measurement was taken. For *Pinus sylvestris*, however, the surface was trimmed with a fresh razor blade to avoid obstruction of tracheids by resin before each measurement. Because resin did not appear to be a major problem for *Pinus pinaster*, we debarked the end of branches of this species to avoid an excessive resin exudation, but did not trim the surface cut each time a measurement was taken.

The rigid silicon tube between the branch end and the pressure sensor functioned as a vacuum reservoir. Firstly, the branch-vacuum reservoir pathway was closed, i.e., the branch end was open to the atmosphere. A pressure of ~40 kPa was obtained in the vacuum reservoir by pulling the syringe plunger. Then, the vacuum reservoir-syringe pathway was closed and the branch-vacuum reservoir pathway opened. The initial pressure (P_i, kPa) was measured immediately after connecting the branch end to the vacuum reservoir. After extracting air from the branch to the vacuum reservoir for 2 min, the final pressure (P_f, kPa) was measured. Branches were bagged in a black plastic bag during the measurements. Two leaves from the branch were then cut and their water potentials were measured with a Scholander pressure chamber (PMS Instrument Company, Albany, OR, USA). Super glue (Loctite 431) was applied to the branch where the leaf petiole was cut to avoid air-entry in the branch. The xylem water potential (Ψ, MPa) was the average of the two leaf water potentials measured. The branch was then detached from the apparatus and dried on the bench. The drying time was between 15 and 30 min for the first two measurements and 1 h or longer for measurements at more negative water potentials. After drying, the branch was bagged in a black plastic bag to equilibrate for 1 h and then connected to the apparatus to start the next measurement. Measurements were ended when the plants showed strong dehydration, such as dry leaves, which was around −6 MPa for several species, and ca −9 MPa for *F. sylvatica*.

According to the ideal gas law, the amount of moles of air (Δn, mol) discharged from the stem in the vacuum reservoir was calculated as follows:

Table 2. List of the *t*-statistics (*t*), the degrees of freedom (df) and the significance values (*P*) of *t*-tests on Ψ_{50} and Ψ_{88} values in the 10 species studied. Xylem embolism resistance was measured using the pneumatic method (Ψ_{50P}, Ψ_{88P}) and flow-centrifuge/hydraulic-bench dehydration (Ψ_{50H}, Ψ_{88H}) methods.

	t-Test between Ψ_{50P} and Ψ_{50H}			*t*-Test between Ψ_{88P} and Ψ_{88H}		
	t	df	*P*	*t*	df	*P*
Alnus glutinosa (L.) Gaertn.	1.156	7	0.286	4.899	7	0.002
Betula pendula Roth	−1.360	9	0.207	−0.529	9	0.610
Carpinus betulus L.	0.169	4.855*	0.872	3.774	4.164*	0.018
Corylus avellana L.	0.425	9	0.681	1.769	9	0.111
Fagus sylvatica L.	−2.311	10	0.043	4.373	10	0.001
Fraxinus excelsior L.	1.709	5	0.148	0.055	5	0.959
Liriodendron tulipifera L.	−0.942	8	0.374	1.115	8	0.297
Pinus pinaster Aiton	−10.811	14	0.000	−2.618	14	0.020
Pinus sylvestris L.	−6.628	8	0.000	0.672	3.757*	0.540
Quercus robur L.	−2.826	6	0.030	−4.299	6	0.005

Values of df with * suggested that the assumption of homogeneity of variance was broken and thus the degree of freedom was reduced. $P < 0.05$ indicated a significant difference.

$$\Delta n = (P_f - P_i)V/RT \quad (1)$$

where V represented the volume of the vacuum reservoir (0.0082 L), R the gas constant (8.314 kPa L mol^{-1} K^{-1}) and T the room temperature. Then, also according to the ideal gas law, the volume of the air discharged (AD, µl) was calculated by transforming Δn to an equivalent volume of air at atmospheric pressure (P_{atm}, 94 kPa at 618 m, the altitude of Ulm University). Any leakage from the apparatus could be calculated from the pressure change over 2 min when the branch-vacuum reservoir pathway was closed. This minor error was then subtracted from AD (the air discharged).

The percentage of air discharged (PAD, %), which was analogous to the percentage loss of conductivity (PLC, %), was calculated as follows:

$$PAD = 100 * (AD_i - AD_{min})/(AD_{max} - AD_{min}) \quad (2)$$

where AD_i was the volume of air discharged at each measurement, AD_{min} the minimum volume of air discharged when the branch was fully hydrated and AD_{max} the maximum volume of air discharged at the lowest xylem water potential. Therefore, the initial air discharged from a fully hydrated stem is considered as a reference point, which accounts for the non-conduit air volume from the pith, intercellular spaces and outside air. If this non-conduit volume does not increase during branch dehydration, the air volume inside the branch would only increase if a new embolism is formed and connected to the cut base and apparatus.

The stem vulnerability curve was then constructed by plotting the PAD and Ψ values with the following function (Pammenter and Vander Willigen 1998):

$$PAD = 100/(1 + \exp((S/25)(\Psi - b))) \quad (3)$$

where S represented the slope of the curve and b was equal to Ψ_{50}, i.e., the xylem water potential at 50% air discharged from the stem. Ψ_{88} (i.e., the xylem water potential at 88% air discharged in the stem) was calculated following Domec and Gartner (2001) as

$$\Psi_{88} = -2/(S/25) + b \quad (4)$$

The hydraulic-bench dehydration method

Stem vulnerability curves of *F. excelsior* and *Q. robur* were constructed using the hydraulic-bench dehydration method since their maximum vessel length was longer than the flow-centrifuge rotor length (28 cm) (Cochard et al. 2005, Li et al. 2015). Data of *F. excelsior* were based on Li et al. (2015), who studied similar sized branches from the same trees as those used for this study.

For *Q. robur*, 15 branches that had a total length between 1.5 and 2 m were collected from six adult trees at the campus of Ulm University in the early morning of August 2017. The samples were wrapped in wet plastic bags and brought to the lab within 15 min. Branches were re-cut under water and rehydrated in water for 1 h to eliminate any potential cutting artefact (Torres-Ruiz et al. 2015). Then, branches were dehydrated in the lab with different time intervals from 1 to 24 h. After bagging the branches for 1 h to create equilibrium between the leaf and xylem water potential, three leaves from the current year stem were cut for water potential measurements using a pressure chamber. The average of the measurements was regarded as the xylem water potential (Ψ). Then, branches were re-cut under water into 3 cm long current year stem segments, which were connected to a modified Sperry apparatus (Sperry et al. 1988) to measure the percentage loss of hydraulic conductivity (PLC, %). Briefly, the distal end of the stem segment was connected to a 60 cm high water column and the proximal end to a pipette via

a silicon tube filled with water. We used demineralized, filtered (0.2 μm) and degassed water with 10 mM KCl and 1 mM $CaCl_2$ for all hydraulic measurements. By measuring the time that was required to fill a volume of 0.01 ml in the pipette, the flow rate of the segment (F, μg s^{-1}) was calculated as the average of three continuous measurements. The hydraulic conductivity of the segment (K_h, kg m s^{-1} MPa^{-1}) was calculated as follows:

$$K_h = F/(P/L) \quad (5)$$

where P represented the water pressure applied to the segment (0.006 MPa) and L (m) was the length of the segment.

Then segments were flushed with water at 120 kPa for 30 min to remove potential emboli, and connected to the Sperry apparatus to obtain the maximum conductivity (K_{max}, kg m s^{-1} MPa^{-1}). The PLC was then calculated as follows:

$$PLC = 100 * (K_{max} - K_h)/K_{max} \quad (6)$$

The stem vulnerability curves were plotted with PLC and Ψ values as mentioned above.

The flow-centrifuge method

The flow-centrifuge technique (Cochard et al. 2005) was applied to the six diffuse-porous angiosperms and two conifer species (Table 1). Branches cut in the early morning were stored at 4 °C in a MICROPUR solution (Katadyn, Wallisellen, Switzerland) and processed within a week. Stem segments of 28 cm length were excised under water with both ends debarked and trimmed, mounted in a custom-built rotor chamber, which uses a commercially available centrifuge as basis (Sorvall RC-5C, Thermo Fisher Scientific, Waltham, MA, USA). The maximum sample conductivity (K_{max}) was first determined at low speed and relatively high xylem pressure (−0.5 MPa). By increasing the rotational velocity, the xylem pressure (Ψ) was decreased stepwise and the hydraulic conductivity (K_h) was measured at each pressure level. The PLC was calculated as Eq. (6) and stem vulnerability curves were plotted as mentioned above.

Statistics

We first tested the Ψ_{50} values determined by the pneumatic method (Ψ_{50P}) across species against those obtained by one of the hydraulic methods (Ψ_{50H}, including the flow-centrifuge or hydraulic-bench dehydration method) using an independent-samples t-test. For the two ring-porous species, a one-sample t-test was used to determine the difference between Ψ_{50P} and Ψ_{50H} values, since only a single vulnerability curve was obtained based on the hydraulic-bench method. In both tests, Ψ_{50} values were considered to be significantly different for a particular species when their 95% confidence intervals did not overlap. Then, we ran a linear regression analysis to test how Ψ_{50H} could be predicted from Ψ_{50P}. Similar t-tests and a regression analysis were also applied to Ψ_{88P} (Ψ_{88} based on the pneumatic method) and Ψ_{88H} (Ψ_{88} based on the flow-centrifuge or hydraulic-bench dehydration method), and to S_P (slope of the percentage of air discharge) and S_H (slope of the percentage loss of hydraulic conductivity). All statistical analyses were done in SPSS 21 (IBM, Armonk, New York, USA) and all figures were made in SigmaPlot 12.5 (Systat Software Inc., Erkrath, Germany).

Results

Vulnerability curves based on the pneumatic method were obtained for the six diffuse-porous species (Figure 1). The 95% confidence bands of the pneumatic curves and hydraulic curves showed considerable overlap, which was especially the case for *B. pendula*. The Ψ_{50P} values of these species showed no difference from the Ψ_{50H} values ($P > 0.05$), except that a marginal difference was found for *F. sylvatica* ($P = 0.04$) (Tables 1 and 2). Ψ_{88P} and Ψ_{88H} values showed significant difference ($P < 0.05$) for *Alnus glutinosa*, *Carpinus betulus* and *F. sylvatica*, but no difference for the other three diffuse-porous species (Tables 1 and 2).

A vulnerability curve based on the pneumatic method could also be obtained for 2-year-old branches of *F. excelsior* (Figure 2a). However, the method could not be successfully applied to 3- to 5-year-old branches of *Q. robur* because the amount of air discharged from fresh samples that were not subject to any drought stress was too high. Hence, the final pressure (P_f) reached atmospheric pressure even when the branch was fully hydrated. Since wide earlywood vessels in *Q. robur* are known to be functional for 1 year only, the xylem of previous growth rings and the pith tissue was glued off at the branch end, with only the xylem from the current growth ring directly exposed to the pneumatic apparatus. This minor modification resulted in vulnerability curves of this species as shown in Figure 2b. Comparison of Ψ_{50P} and Ψ_{50H} for the two ring-porous species showed a 0.3 MPa difference for *F. excelsior* and 0.4 MPa difference for *Q. robur*. A significant difference was found for *Q. robur* ($P = 0.03$), but not for *F. excelsior* ($P = 0.15$). Similarly, a significant difference between the Ψ_{88P} and Ψ_{88H} values was found for *Q. robur* ($P < 0.01$), but not for *F. excelsior* ($P = 0.96$) (Table 1).

The vulnerability curves for the two conifer species showed a large difference between the pneumatic and hydraulic method (Figure 2c and d). The Ψ_{50P} and Ψ_{50H} values differed significantly ($P < 0.01$) by 0.9 and 1.2 MPa for *P. pinaster* and *P. sylvestris*, respectively, while Ψ_{88P} and Ψ_{88H} values differed for *P. pinaster* ($P = 0.02$) and showed no difference for *P. sylvestris* ($P = 0.54$) (Table 1).

Ψ_{50} values from the pneumatic (Ψ_{50P}) and hydraulic curves (Ψ_{50H}) were strongly correlated ($R^2 = 0.670$, $P < 0.01$; Figure 3a). The fitted line was $\Psi_{50H} = 0.945\Psi_{50P} - 0.383$, which was close to the 1:1 line (Figure 3a). A stronger correlation was obtained when analysing the six diffuse-porous

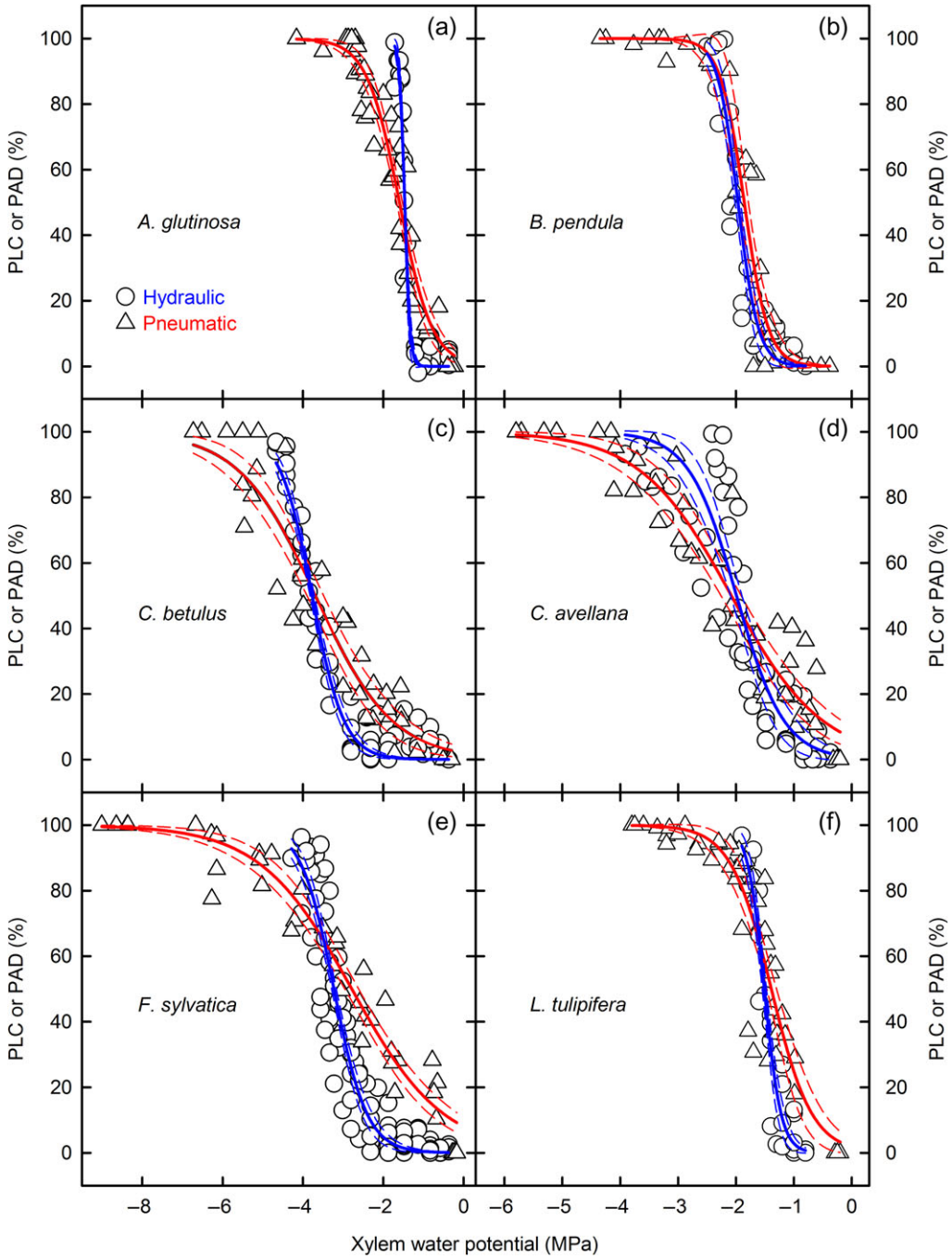

Figure 1. Stem vulnerability curves of six diffuse-porous species. Circles and blue solid lines represent data and regression fits based on the hydraulic method. Triangles and red solid lines represent data and regression lines obtained with the pneumatic method. The short dash lines represent 95% confidence bands.

species ($R^2 = 0.957$, $P < 0.01$), and the eight angiosperm species ($R^2 = 0.911$, $P < 0.01$). Two conifers (*P. pinaster* and *P. sylvestris*) did not fall within the 95% confidence band (Figure 3a).

Ψ_{88P} and Ψ_{88H} were also strongly correlated ($R^2 = 0.752$, $P < 0.01$; Figure 3b). The fitted line was $\Psi_{88H}=0.733\Psi_{88P} - 0.492$, which was close to the 1:1 line (Figure 3b). A higher correlation also occurred when analysing the six diffuse-porous species separately ($R^2 = 0.950$, $P < 0.01$), as well as the eight angiosperm species ($R^2 = 0.876$, $P < 0.01$). Only *P. pinaster* did not fall within the 95% confidence bands (Figure 3b).

The slope of the percentage of air discharge (S_P) was not significantly correlated with the slope of the percentage loss of hydraulic conductivity (S_H) ($R^2 = 0.198$, $P = 0.20$). When *A. glutinosa* was excluded as an outlier, however, a significant correlation was shown ($R^2 = 0.566$, $P = 0.02$) (Figure 3c).

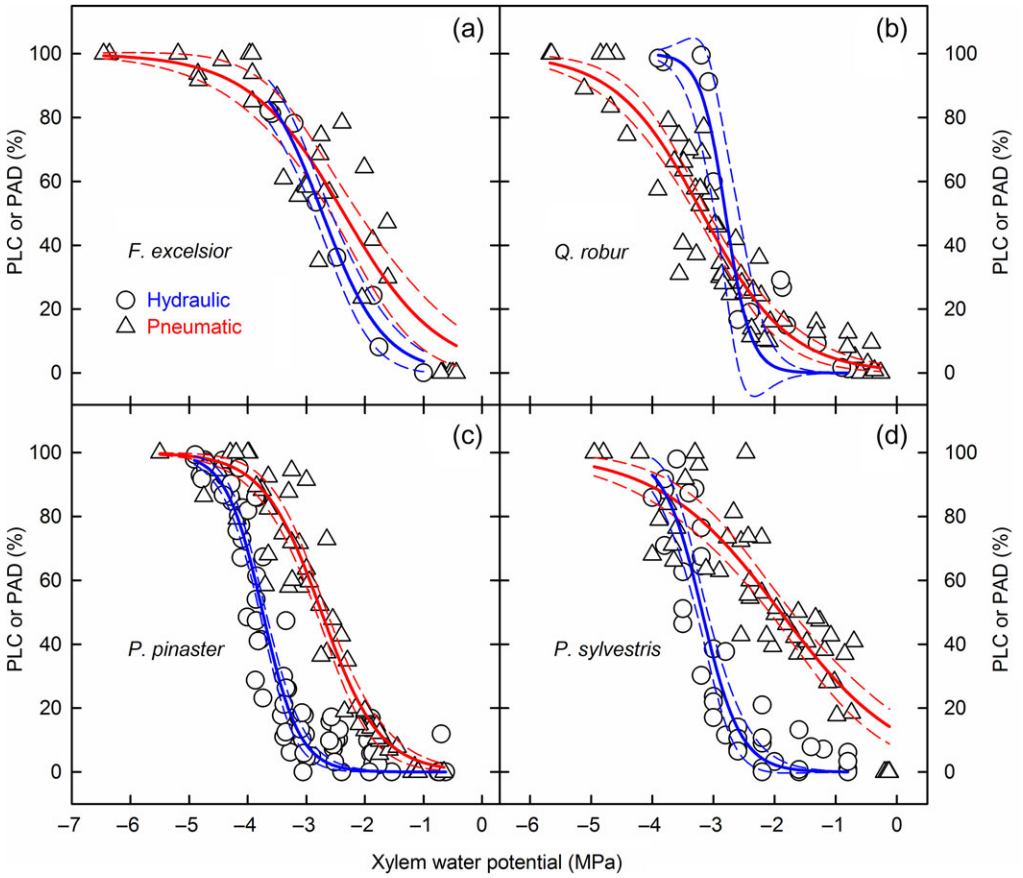

Figure 2. Stem vulnerability curves of two ring-porous species (a, b) and two conifer species (c, d). Circles and blue solid lines represent data and regression fits from the hydraulic-bench dehydration (a, b) or flow-centrifuge method (c, d). Triangles and red solid lines represent data and regression lines from the pneumatic method. The short dash lines represent 95% confidence bands. Bench dehydration data of *F. excelsior* were reproduced from Li et al. (2015). Pneumatic data for *Q. robur* required gluing off xylem from the previous growth rings.

Excluding *A. glutinosa*, the solid line showed the fitting: $S_H = 0.822S_P + 64.792$, while *F. excelsior* and *Liriodendron tulipifera* did not fall within the 95% confidence bands (Figure 3c).

Discussion

Vulnerability curves based on the pneumatic method were largely similar to those based on the hydraulic methods for most angiosperm species, with the exception of the two conifer species studied. Therefore, this finding validates the pneumatic method for temperate angiosperm species and is in agreement with a comparison of the pneumatic method and the hydraulic-bench dehydration method for mainly tropical and subtropical species (Pereira et al. 2016). However, significant differences between Ψ_{50P} and Ψ_{50H} for two out of eight angiosperm species studied (i.e., *F. sylvatica* and *Q. robur*) suggest that the pneumatic method may provide a relative approach to quantify embolism resistance, while there may not be an absolute, standard way to determine Ψ_{50} values for a broad taxonomic range of species. Care should especially be taken for ring-porous species, which can show highly variable vulnerability curves depending on the method applied (Choat et al. 2010, Jacobsen and Pratt 2012, Hacke et al. 2015, Torres-Ruiz et al. 2017).

Agreement between the pneumatic method and flow-centrifuge method was highest for the six diffuse-porous angiosperms. The highest coefficients of correlation (R^2) were found for both Ψ_{50} and Ψ_{88} values. Hence, the pneumatic method appears to be reliable for constructing vulnerability curves of diffuse-porous angiosperms, which are known to show functional vessels over various growth rings (Umebayashi et al. 2010, Sano et al. 2011). This finding also suggests that most of the air discharged during dehydration corresponds to the amount of embolized conduits. While air can also be taken up through the bark and the leaves, the amount of external air was shown to be negligible within a time frame of 2 min (Pereira et al. 2016). Air diffusion via bark and leaf tissue is most likely a slow process, because the resistance of air flow was found to be considerably higher across the periderm, cambium and mesophyll cells than through lumen conduits and interconduit pit membranes (Comstock 1970, Sorz and Hietz 2006, Pereira et al. 2016). Air flow through bordered pit membranes may increase during dehydration and can be explained by pit

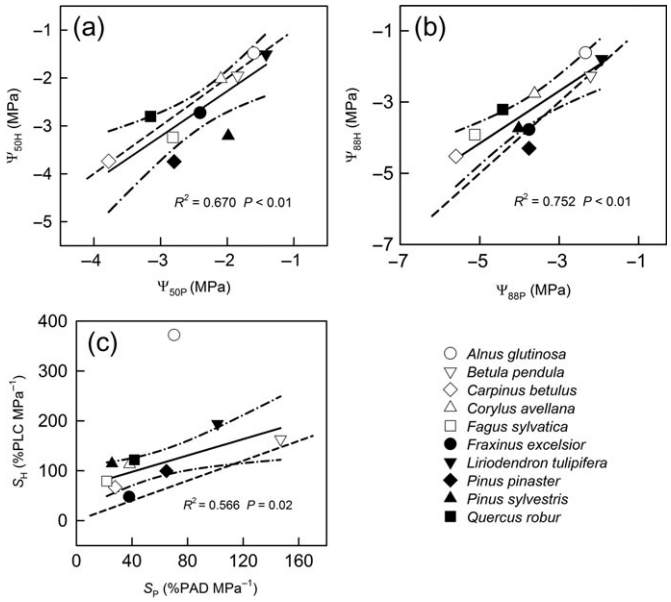

Figure 3. Relationships between Ψ_{50} (a), Ψ_{88} (b) and slope (c) values obtained from the pneumatic curves and the hydraulic curves. (a) Ψ_{50} values of the pneumatic method (Ψ_{50P}) and Ψ_{50} values of the hydraulic method (Ψ_{50H}) were strongly correlated ($R^2 = 0.670$, $P < 0.01$). The solid line showed the fitting: $\Psi_{50H} = 0.945\Psi_{50P} - 0.383$. (b) Ψ_{88} values of the pneumatic method (Ψ_{88P}) and Ψ_{88} values of the hydraulic method (Ψ_{88H}) were strongly correlated ($R^2 = 0.752$, $P < 0.01$). The solid line showed the fitting: $\Psi_{88H} = 0.733\Psi_{88P} - 0.492$. (c) The slope of the percentage of air discharge (S_P) and the slope of the percentage loss of hydraulic conductivity (S_H) were strongly correlated ($R^2 = 0.566$, $P = 0.02$) when excluding *A. glutinosa* as an outlier. The solid line showed the fitting: $S_H = 0.822S_P + 64.792$. Data from different species were presented with different symbols. Dash-dotted lines represented the 95% confidence band. The dash line was the 1:1 line.

membrane shrinkage that is associated with increased porosity (Cohen et al. 2003, Pan et al. 2015, Zhang et al. 2017).

An interesting difference was found between the two ring-porous species studied, including 2-year-old branches of *F. excelsior*, and 3- to 5-year-old branches of *Q. robur*. Since it is known that wide, earlywood vessels in ring-porous species remain only functional over a single season and do not refill (Cochard and Tyree 1990, Cochard et al. 1997, Sano et al. 2011), the amount of gas that can be extracted from embolized earlywood vessels can be high. While working with current-year shoots might provide a solution to avoid this problem, the proportion of lignified xylem tissue to non-xylem tissue can be too small and may not provide sufficient mechanical support for applying the pneumatic method. In addition, the amount of leaves on current year shoots can be small, which would make repeated water potential measurements difficult. Gluing off previous growth rings, as done for *Q. robur*, could provide an alternative, easy solution, especially when dealing with multi-year branches.

Ψ_{50} values showed a significant difference between the pneumatic and flow-centrifuge method for the conifer species tested (Table 1, Figures 2c and d). Although the correlation between Ψ_{50P} and Ψ_{50H} (Figure 3a) and between Ψ_{88P} and Ψ_{88H} (Figure 3b) was significant in all species, it became weaker when the two conifer species were included. The finding of reduced embolism resistance for both conifers is largely in agreement with the two conifer species studied by Pereira et al. (2016). In this study, the difference in Ψ_{50} values between the pneumatic and hydraulic method was 2.4 MPa for *C. sempervirens* and 2.6 MPa for *T. plicata*. Overall, these data suggest a reduced embolism resistance based on the pneumatic method for *P. sylvestris*, *P. pinaster* and *C. sempervirens*, but an increased embolism resistance for *T. plicata*.

Resin in gymnosperm xylem may not be the main reason for the large discrepancy between Ψ_{50P} and Ψ_{50H}, because resin canals are absent in the xylem of *C. sempervirens* and *T. plicata* (Wagenführ 2007, Cleary and Holmes 2011). Moreover, carefully trimming the cut surface of *P. sylvestris* did not seem to provide a shift towards more negative Ψ_{50} values. A possible explanation could be aspiration of the torus-margo pit membrane in conifers (Bouche et al. 2014). When a pit membrane is subject to a certain pressure difference between neighbouring tracheids, the torus could become aspirated and blocks off the pit aperture, preventing air flow from one tracheid to another (Cochard et al. 2009, Jansen et al. 2012). The pressure difference required to cause pit membrane aspiration in conifers was found to range from 0.01 MPa to 0.3 MPa (Bouche et al. 2014, 2015), which means that aspiration is likely when measuring AD_{min} values of conifer branches. Thus, pit membrane aspiration might underestimate the amount of air discharged during a pneumatic measurement, and the maximum PAD would be reached at a less negative water potential, which underestimates xylem embolism resistance. For the same reason, the application of the flow-centrifuge may result in a shift towards less negative Ψ_{50} values if the flow difference across the two sample ends is too high, resulting in pit aspiration (Beikircher et al. 2010, Bouche et al. 2015). Nevertheless, this hypothesis does not explain the more negative Ψ_{50} value for *T. plicata* as reported by Pereira et al. (2016). While further research is needed to test the pneumatic method on additional conifer species, the available evidence indicates that this method is not recommended for gymnosperms.

In conclusion, the pneumatic method may provide considerable advantages over other methods when studying xylem resistance to embolism of temperate angiosperm branches. Compared with hydraulic methods, extracting gas from terminal branch endings is fast and easy. Pneumatic vulnerability curves of several species can be constructed simultaneously within 2 to 3 days, depending on how fast branches dry at room temperature. This method may especially be useful for field measurements at remote locations, student projects, and when dealing with a large number of samples.

Acknowledgments

We thank Peter Zindl and Markus Wespel (Botanical Garden of Ulm University) for support with collecting samples. Y.Z. and S.L. acknowledge financial support from the China Scholarship Council (CSC).

Conflict of interest

We declare that we have no conflict of interest.

Funding

L.J.L. was supported by a post-doctoral fellowship from the Excellence Initiative Program of Université de Bordeaux (UB101 CR1024-R s/CR1024-6M).

References

Anderegg WRL, Klein T, Bartlett M, Sack L, Pellegrini A, Choat B, Jansen S (2016) Meta-analysis reveals that hydraulic traits explain cross-species patterns of drought-induced tree mortality across the globe. Proc Natl Acad Sci USA 113:5024–5029.

Beikircher B, Ameglio T, Cochard H, Mayr S (2010) Limitation of the cavitron technique by conifer pit aspiration. J Exp Bot 61:3385–3393.

Bouche PS, Larter M, Domec JC, Burlett R, Gasson P, Jansen S, Delzon S (2014) A broad survey of hydraulic and mechanical safety in the xylem of conifers. J Exp Bot 65:4419–4431.

Bouche PS, Jansen S, Cochard H, Burlett R, Capdeville G, Delzon S (2015) Embolism resistance of conifer roots can be accurately measured with the flow-centrifuge method. J Plant Hydraulics 2:1–9.

Brodribb TJ, Bienaimé D, Marmottant P (2016*a*) Revealing catastrophic failure of leaf networks under stress. Proc Natl Acad Sci USA 113: 4865–4869.

Brodribb TJ, Skelton RP, McAdam SA, Bienaimé D, Lucani CJ, Marmottant P (2016*b*) Visual quantification of embolism reveals leaf vulnerability to hydraulic failure. New Phytol 209:1403–1409.

Brodribb TJ, Carriqui M, Delzon S, Lucani C (2017) Optical measurement of stem xylem vulnerability. Plant Physiol 174:2054–2061.

Charrier G, Torres-Ruiz JM, Badel E et al. (2016) Evidence for hydraulic vulnerability segmentation and lack of xylem refilling under tension. Plant Physiol 172:1657–1668.

Choat B, Drayton WM, Brodersen C, Matthews MA, Shackel KA, Wada H, Mcelrone AJ (2010) Measurement of vulnerability to water stress-induced cavitation in grapevine: a comparison of four techniques applied to a long-vesseled species. Plant Cell Environ 33:1502–1512.

Choat B, Jansen S, Brodribb TJ et al. (2012) Global convergence in the vulnerability of forests to drought. Nature 491:752–755.

Choat B, Badel E, Burlett R, Delzon S, Cochard H, Jansen S (2016) Noninvasive measurement of vulnerability to drought induced embolism by X-ray microtomography. Plant Physiol 170:273–282.

Cleary MR, Holmes T (2011) Formation of traumatic resin ducts in the phloem of western redcedar (*Thuja plicata*) roots following abiotic injury and pathogenic invasion by *Armillaria ostoyae*. IAWA J 32: 351–359.

Cochard H, Delzon S (2013) Hydraulic failure and repair are not routine in trees. Ann For Sci 70:659–661.

Cochard H, Tyree MT (1990) Xylem dysfunction in *Quercus*: vessel sizes, tyloses, cavitation and seasonal changes in embolism. Tree Physiol 6:393–407.

Cochard H, Cruiziat P, Tyree MT (1992) Use of positive pressures to establish vulnerability curves: further support for the air-seeding hypothesis and implications for pressure-volume analysis. Plant Physiol 100:205–209.

Cochard H, Peiffer M, Le Gall K, Granier A (1997) Developmental control of xylem hydraulic resistances and vulnerability to embolism in *Fraxinus excelsior* L.: impacts on water relations. J Exp Bot 48:655–663.

Cochard H, Damour G, Bodet C, Tharwat I, Poirier M, Améglio T (2005) Evaluation of a new centrifuge technique for rapid generation of xylem vulnerability curves. Physiol Plant 124:410–418.

Cochard H, Holtta T, Herbette S, Delzon S, Mencuccini M (2009) New insights into the mechanisms of water-stress-induced cavitation in conifers. Plant Physiol 151:949–954.

Cochard H, Herbette S, Barigah T, Badel E, Ennajeh M, Vilagrosa A (2010) Does sample length influence the shape of xylem embolism vulnerability curves? A test with the Cavitron spinning technique. Plant Cell Environ 33:1543–1552.

Cochard H, Badel E, Herbette S, Delzon S, Choat B, Jansen S (2013) Methods for measuring plant vulnerability to cavitation: a critical review. J Exp Bot 64:4779–4791.

Cohen S, Bennink JP, Tyree MT (2003) Air method measurements of apple vessel length distributions with improved apparatus and theory. J Exp Bot 54:1889–1897.

Comstock GL (1970) Directional permeability of softwoods. Wood Fiber Sci 1:283–289.

Crombie DS (1983) The physiology of the cavitation of xylem sap. PhD thesis, Glasgow University, Glasgow, UK.

Domec JC, Gartner BL (2001) Cavitation and water storage capacity in bole xylem segments of mature and young Douglas-fir trees. Trees 15:204–214.

Ellmore GS, Ewers FW (1985) Hydraulic conductivity in trunk xylem of elm, *Ulmus americana*. IAWA Bull 6:303–307.

Ellmore GS, Ewers FW (1986) Fluid flow in the outermost xylem increment of a ring-porous tree, *Ulmus americana*. Am J Bot 73: 1771–1774.

Ennajeh M, Simões F, Khemira H, Cochard H (2011) How reliable is the double-ended pressure sleeve technique for assessing xylem vulnerability to cavitation in woody angiosperms? Physiol Plant 142: 205–210.

Espino S, Schenk HJ (2011) Mind the bubbles: achieving stable measurements of maximum hydraulic conductivity through woody plant samples. J Exp Bot 62:1119–1132.

Hacke UG, Venturas MD, MacKinnon ED, Jacobsen AL, Sperry JS, Pratt RB (2015) The standard centrifuge method accurately measures vulnerability curves of long-vesselled olive stems. New Phytol 205: 116–127.

Hochberg U, Windt CW, Ponomarenko A, Zhang Y-J, Gersony J, Rockwell FE, Holbrook NM (2017) Stomatal closure, basal leaf embolism and shedding protect the hydraulic integrity of grape stems. Plant Physiol 174:764–775.

Jacobsen AL, Pratt RB (2012) No evidence for an open vessel effect in centrifuge-based vulnerability curves of a long-vesseled liana (*Vitis vinifera*). New Phytol 194:982–990.

Jacobsen AL, Pratt RB, Davis SD, Tobin MF (2014) Geographic and seasonal variation in chaparral vulnerability to cavitation. Madroño 61: 317–327.

Jansen S, Lamy J-B, Burlett R, Cochard H, Gasson P, Delzon S (2012) Plasmodesmatal pores in the torus of bordered pit membranes affect cavitation resistance of conifer xylem. Plant Cell Environ 35: 1109–1120.

Jansen S, Schuldt B, Choat B (2015) Current controversies and challenges in applying plant hydraulic techniques. New Phytol 205: 961–964.

Li S, Feifel M, Karimi Z, Schuldt B, Choat B, Jansen S (2015) Leaf gas exchange performance and the lethal water potential of five European species during drought. Tree Physiol 36:179–192.

Li Y, Sperry JS, Taneda H, Bush SE, Hacke UG (2008) Evaluation of centrifugal methods for measuring xylem cavitation in conifers, diffuse- and ring-porous angiosperms. New Phytol 177:558–568.

Mayr S, Rosner S (2011) Cavitation in dehydrating xylem of *Picea abies*: energy properties of ultrasonic emissions reflect tracheid dimensions. Tree Physiol 31:59–67.

OpenSourceOV (2018) Community-driven resources for measuring drought tolerance in drought. http://www.opensourceov.org/ (18 January 2018, date last accessed).

Pan R, Geng J, Cai J, Tyree MT (2015) A comparison of two methods for measuring vessel length in woody plants. Plant Cell Environ 38: 2519–2526.

Pammenter NW, Vander Willigen C (1998) A mathematical and statistical analysis of the curves illustrating vulnerability of xylem to cavitation. Tree Physiol 18:589–593.

Pereira L, Bittencourt PRL, Oliveira RS, Junior MBM, Barros FV, Ribeiro RV, Mazzafera P (2016) Plant pneumatics: stem air flow is related to embolism – new perspectives on methods in plant hydraulics. New Phytol 211:357–370.

Salleo S, Hinckley TM, Kikuta SB, Lo Gullo MA, Weilgony P, Yoon TM, Richter H (1992) A method for inducing xylem emboli in situ: experiments with a field-grown tree. Plant Cell Environ 15:491–497.

Sano Y, Morris H, Shimada H, Ronse De Craene LP, Jansen S (2011) Anatomical features associated with water transport in imperforate tracheary elements of vessel-bearing angiosperms. Ann Bot 107:953–967.

Scoffoni C, Jansen S (2016) I can see clearly now–embolism in leaves. Trends Plant Sci 21:723–725.

Sperry JS (1986) Relationship of xylem embolism to xylem pressure potential, stomatal closure, and shoot morphology in the palm *Rhapis excelsa*. Plant Physiol 80:110–116.

Sperry JS, Tyree MT (1988) Mechanism of water stress-induced xylem embolism. Plant Physiol 88:581–587.

Sperry JS, Donnelly JR, Tyree MT (1988) A method for measuring hydraulic conductivity and embolism in xylem. Plant Cell Environ 11:35–45.

Sorz J, Hietz P (2006) Gas diffusion through wood: implications for oxygen supply. Trees 20:34–41.

Torres-Ruiz JM, Cochard H, Mayr S, Beikircher B, Diaz-Espejo A, Rodriguez-Dominguez CM, Badel E, Fernández JE (2014) Vulnerability to cavitation in *Olea europaea* current-year shoots: further evidence of an open vessel artefact associated with centrifuge and air-injection techniques. Physiol Plant 152:465–474.

Torres-Ruiz JM, Jansen S, Choat B et al. (2015) Direct micro-CT observation confirms the induction of embolism upon xylem cutting under tension. Plant Physiol 167:40–43.

Torres-Ruiz JM, Cochard H, Choat B et al. (2017) Xylem resistance to embolism: presenting a simple diagnostic test for the open vessel artefact. New Phytol 215:489–499.

Tyree MT, Dixon MA (1986) Water stress induced cavitation and embolism in some woody plants. Physiol Plant 66:397–405.

Tyree MT, Sperry JS (1989) Vulnerability of xylem to cavitation and embolism. Annu Rev Plant Phys 40:19–38.

Tyree MT, Zimmermann MH (eds) (2002) Xylem structure and the ascent of sap. Springer, Berlin.

Umebayashi T, Utsumi Y, Koga S, Inoue S, Matsumura J, Oda K, Fujikawa S, Arakawa K, Otsuki K (2010) Xylem water-conducting patterns of 34 broadleaved evergreen trees in Southern Japan. Trees 24: 571–583.

Wagenführ R (ed) (2007) Holzatlas. Carl Hanser, Leipzig, Germany.

Wang R, Zhang L, Zhang S, Cai J, Tyree MT (2014) Water relations of *Robinia pseudoacacia* L.: do vessels cavitate and refill diurnally or are R-shaped curves invalid in *Robinia*? Plant Cell Environ 37: 2667–2678.

Wheeler JK, Huggett BA, Tofte AN, Rockwell FE, Holbrook NM (2013) Cutting xylem under tension or supersaturated with gas can generate PLC and the appearance of rapid recovery from embolism. Plant Cell Environ 36:1938–1949.

Wolkerstorfer SV, Rosner S, Hietz P (2012) An improved method and data analysis for ultrasound acoustic emissions and xylem vulnerability in conifer wood. Physiol Plant 146:184–191.

Zhang Y, Klepsch M, Jansen S (2017) Bordered pits in xylem of vesselless angiosperms and their possible misinterpretation as perforation plates. Plant Cell Environ 40:2133–2146.